



Robust adaptive neural networks control for dynamic positioning of ships with unknown saturation and time-delay

Kun Liang^{a,b,*}, Xiaogong Lin^a, Yu Chen^b, Yeye Liu^a, Zhaoyu Liu^b, Zhengxiang Ma^b, Wenli Zhang^b

^a College of Automation, Harbin Engineering University, No. 145 Nantong Street, Nangang District, Harbin City, Heilongjiang Province, China

^b School of Intelligent Engineering, Zhengzhou University of Aeronautics, No. 15 Wenyuan West Road, Zhengzhou City, Henan Province, China

ARTICLE INFO

Keywords:

Time delay
Dynamic positioning of ships
Unknown saturation
Minimal-parameter-learning
Robust adaptive control

ABSTRACT

In this paper, a robust adaptive neural networks control based on minimal-parameter-learning (MLP) is proposed for dynamic positioning (DP) of ships with unknown saturation, time delay, external disturbance and dynamic uncertainties. Through the velocities backstepping method, radial basis function (RBF) neural networks and robust adaptive control are incorporated to design a novel controller of which an appropriate Lyapunov-Krasovskii Function (LKF) is constructed to overcome the effect caused by time-delay. Meanwhile, the MLP technology is applied to reduce the computational burden while only one parameter need to be update by an adaptive law. In additional, a robust adaptive compensate term is introduced to estimate the bound of the lumped disturbance including the unknown saturation, unknown external disturbance and the approximate error of neural networks control while the robustness of MLP is improved and the unknown saturation is compensated. The developed control law makes the DP closed-loop system be uniformly ultimately stable which can be proved strictly through Lyapunov theory. Finally, simulations with a guidance law are proposed to demonstrate the validity of controller we developed.

1. Introduction

With the increasing reliance on oceans exploitation in a spectrum of human activities, the research for advance marine mechatronic systems is attracting more and more attention. Dynamic positioning (DP) system is a sort of typical marine mechatronic system from a control perspective for surface vessels and is essential for many marine applications, such as drilling, pipe-laying, and diving support [1]. With the advances of the nonlinear control, the DP nonlinear control has gradually gained much attention and various approaches have been used for DP systems to achieve better performance, such as adaptive control [2], hybrid control [3], robust control [4] fault-tolerate control [5] and etc. [6].

Input saturation [7,8], giving rise to degraded performance and even instability of the DP control system, is a potential problem for the DP system since the commanded control inputs calculated by the DP controller are possibly constrained by the maximum forces and moment that the propulsion system can produce [9]. In [10], Hu Xin et al. proposed a robust dynamic surface control strategy where an auxiliary dynamic system to handle input saturation. Perez and Donaire proposed

DP proportional-integral control, where disturbances and input saturation were handled by the integral action with anti-windup scheme [11]. On the other hand, the priori knowledge of vessel dynamics is difficult to be exactly determined since the vessel dynamics is related to constantly varying operational conditions. To handle with the model parameter uncertainties, Do [12] developed a DP robust adaptive output feedback control law with an adaptive observer using vectorial backstepping method. Du et al. [13] designed a DP robust NN control law combining adaptive NNs with vectorial backstepping method, where NN approximators were applied to compensate for unknown vessel dynamics and disturbances in the DP control law. To deal with the known input saturation and dynamic uncertainties, simultaneously, a robust adaptive neural network control law [14] is developed through incorporating adaptive radial basis function (RBF) NNs, an auxiliary dynamic system and a robust control term into dynamic surface control method. In our previous work [15], a finite-time anti-windup controller is developed and the finite-time convergence is guaranteed while the saturation and velocity-free are considered. Furthermore, a novel robust adaptive multistage anti-windup dynamic surface control is designed in [16] for

* Corresponding author.

E-mail address: drliangkun@126.com (K. Liang).

<https://doi.org/10.1016/j.apor.2021.102609>

Received 6 November 2020; Received in revised form 7 February 2021; Accepted 1 March 2021

Available online 13 March 2021

0141-1187/© 2021 Elsevier Ltd. All rights reserved.

dynamic positioning ship with saturation, while the overshoot is reduced in some degree. However, the actuator performance maybe unknown in practice [17,18] while most of mentioned researches are based on the assumption that the input saturation is known and it is the first motivation of this paper.

In addition, time delay is encountered in many dynamical systems and often leads to performance deterioration which engender interest in this topic has been growing strongly in recent decades. In the DP system, the main kind of time delay is encountered in actuators, while another obvious kind of delay is the one produced between the sensors and the activation of the control mechanism [19,20]. In [21], time-varying input delay is considered based on the linearized dynamic positioning system and a finite-time controller with transient is provided while the nonlinear characters is neglected. In [22], a fuzzy controller is proposed while time delay and dynamic uncertainties are considered simultaneously based on the nonlinear model. Unfortunately, it should be point out that two drawbacks lies in the results of [22]: 1). The input saturation is neglected which makes it hard to apply the controller in engineering practice while the constraint of power provided by actuators is inevitable; 2). The computational burden of fuzzy control is increasing to achieve a better approximation result. Thus, the second motivation and the difficult point of the paper are how to design a dynamic positioning control with dynamic uncertainties, unknown disturbance, unknown input saturation and time delay at the cost of less computational burden while a better control performance can be achieved simultaneously.

According to the aforementioned discussion, it is the first time in the literature that unknown time-varying disturbances, time delay, unknown input saturation, dynamic uncertainties are simultaneously dealt with in the DP control design. A MLP-based robust adaptive controller is proposed through incorporating robust adaptive compensated technology [13], MLP technology [23], Lyapunov–Krasovskii theory [24] and RBFNN [25] into backstepping control. An appropriate Lyapunov–Krasovskii Function (LKF) is constructed to overcome the effect caused by time-delay and the MLP technology is applied to reduce the computational burden while only one parameter need to be update by an adaptive law. In additional, a robust adaptive compensate term is introduced to estimate the bound of the lumped disturbance including the unknown saturation, unknown external disturbance and the approximate error of neural networks control while the robustness of MLP is improved and the unknown saturation is compensated. The developed control law makes the DP closed-loop system be uniformly ultimately stable which can be proved strictly through Lyapunov theory. Finally, simulations with a guidance law are proposed to demonstrate the validity of controller we developed. Comparing with the result in [13, 22], the main contributions are two aspects:

- (1) To the best knowledge of authors, it is the first time in the literature that the unknown input saturation, time delay, unknown time-varying disturbances and dynamic uncertainties are considered simultaneously in dynamic positioning controller design.
- (2) A robust adaptive neural networks control based on MLP is proposed for dynamic positioning of ships, so the problems of “explosion of complexity” in the conventional backstepping method and “curse of dimensionality” in the traditional neural networks control are avoided while the robustness of RBFNN with MLP is improved since the estimation error can be compensated by the robust adaptive term. In additional, the prior knowledge of input

saturation is not required which means the controller we developed can be applied on more scenarios.

The remainder of the paper is organized as follows: In Section 2, the problem formulation of control is detailed for vessels. Following in Section 3, the control strategy is proposed and the stability analysis is provided. The vessel dynamics and the proposed control schemes are simulated in Section 4, and concluding remarks are made in Section 5.

2. Problem formulation

At first, DP system model with time delay and unknown input saturation can be described as [24,26,27]

$$\dot{\eta} = J(\psi)v \quad (1)$$

$$M\dot{v} + (C(v) + D(v))v = \Delta f(\eta(t-d), v(t-d)) + sat(\tau) + \tau_d \quad (2)$$

$$y = \eta \quad (3)$$

Where $\Delta f(\eta(t-d), v(t-d))$ is an unknown function containing delay states and can be defined $\Delta f(\eta(t-d), v(t-d)) = \Delta f(t-d)$ while d is a known constant. M denotes inertia matrix and is positive defining. $C(v)$ denotes Coriolis matrix and $D(v)$ is hydrodynamic damping matrix including linear terms and nonlinear terms. $J(\psi)$ is the rotation matrix given by

$$J(\psi) = \begin{bmatrix} \cos(\psi) & -\sin(\psi) & 0 \\ \sin(\psi) & \cos(\psi) & 0 \\ 0 & 0 & 1 \end{bmatrix} \quad (4)$$

τ_d represents the lumped disturbance. $sat(\tau) = [sat(\tau_1), sat(\tau_2), sat(\tau_3)]^T$ represents the constrained control input vector produced by propeller and thruster system, consisting of force τ_1 in surge, force τ_2 in sway and moment τ_3 in yaw. The relationship between the desired control input and the actual control input can be described as:

$$\Delta\tau = sat(\tau) - \tau \quad (5)$$

Where $\Delta\tau$ denotes the difference between the desired control input τ and the actual control input $sat(\tau)$. Define $G(t) = \tau_d + \Delta\tau$ and the dynamic model of dynamic positioning systems can be rewritten as:

$$\dot{\eta} = J(\psi)v \quad (6)$$

$$\dot{v} = -\frac{1}{M}(C(v) + D(v))v + \frac{\Delta f(t-d)}{M} + \frac{1}{M}\tau + \frac{G(t)}{M} \quad (7)$$

$$y = \eta \quad (8)$$

Without loss of generality, some assumptions are introduced first:

Assumption 1. The parameters M , $D(v)$ and $C(v)$ are unknown, yet $M^T = M$.

Assumption 2. The lumped disturbance $G(t) = (g_1(t), g_2(t), g_3(t))^T$ is unknown yet bounded and there exists unknown positive constants \bar{G} such that

$$\|G(t)\| \leq \bar{G} < \infty, i = 1, 2, 3 \quad (9)$$

Assumption 3. [27]: The nonlinear functions $\Delta f(t-d)$ satisfy the following condition:

$$\|\Delta f(\eta, v)\| \leq \bar{f} \quad (10)$$

Where \bar{f} is a known smooth function.

Remark 1. Since the ocean environment is constantly changing and has finite energy, the disturbances acting on the ship can be viewed as the unknown time-varying yet bounded signals. Therefore, **Assumption 2** is reasonable.

The control objective in this paper is to design a dynamic positioning robust nonlinear control law τ for the ship with unknown input saturation, time delay, unknown time-varying disturbances and dynamic uncertainties, so that the ship's position (x, y) and heading ψ are maintained at the desired values $\eta_d = (x_d, y_d, \psi_d)^T$ with arbitrarily small errors, while all signals in the dynamic positioning closed-loop control system are uniformly ultimately boundedness.

3. Main results

3.1. Robust adaptive neural networks control design

In this subsection, a MLP-based robust adaptive controller is designed for dynamic positioning of ships with time delay, unknown input saturation, unknown time-varying disturbances and dynamic uncertainties through incorporating robust adaptive compensated technology, MLP technology, Lyapunov – Krasovskii theory and RBFNN into backstepping control. The DP control design consists of the following six steps.

Step 1. Define the position error surface vector and velocity error surface vector as following:

$$z_1 = \eta - \eta_d \quad (11)$$

$$z_2 = v - \alpha \quad (12)$$

Select the Lyapunov function candidate as following:

$$V_1 = \frac{1}{2} z_1^T z_1 \quad (13)$$

Taking the time derivative for V_1 :

$$\begin{aligned} \dot{V}_1 &= z_1^T \dot{z}_1 \\ &= z_1^T (J(\psi)(z_2 + \alpha) - \dot{\eta}_d) \end{aligned} \quad (14)$$

Design the intermediate control function vector:

$$\alpha = -J^T(\psi) (K_1 z_1 - \dot{\eta}_d) \quad (15)$$

Where the $K_1 \in \mathbb{R}^{3 \times 3}$ is a positive-definite design matrix and the \dot{V}_1 can be rewritten as:

$$\begin{aligned} \dot{V}_1 &= z_1^T \dot{z}_1 \\ &= z_1^T J(\psi) (z_2 - J^T(\psi) K_1 z_1) \\ &= -z_1^T K_1 z_1 + z_1^T J(\psi) z_2 \end{aligned} \quad (16)$$

Step 2. Taking the time derivative of z_2 is

$$\begin{aligned} \dot{z}_2 &= \dot{v} - \dot{\alpha} \\ &= -\frac{C(v) + D(v)}{M} v + \frac{\Delta f(t-d)}{M} + \frac{1}{M} \tau(t) + \frac{1}{M} G(t) - \dot{\alpha} \end{aligned} \quad (17)$$

To compensate the effect of time delay, Lyapunov-Krasovskii function is constructed as followings [24]

$$V_2 = V_1 + \frac{1}{2} z_2^T M z_2 + \int_{t-d}^t \Phi(\rho) d\rho \quad (18)$$

Where $\int_{t-d}^t \Phi(\rho) d\rho$ is a positive function designed afterwards and define $\Phi(\eta(t), v(t)) = \Phi(t) \Delta f(\eta(t), v(t)) = \Delta f(t)$. Taking the time derivative of V_2 is

$$\begin{aligned} \dot{V}_2 &= \dot{V}_1 + z_2^T M \dot{z}_2 + \Phi(t) - \Phi(t-d) \\ &= -z_1^T K_1 z_1 + z_1^T J(\psi) z_2 + \Phi(t) \\ &\quad - \Phi(t-d) + z_2^T (- (C(v) + D(v)) v + \Delta f(t-d) + \tau(t) + G(t) - M\dot{\alpha}) \\ &= -z_1^T K_1 z_1 + z_1^T J(\psi) z_2 + z_2^T \Delta f(t-d) - \Phi(t-d) \\ &\quad + z_2^T (- (C(v) + D(v)) v + \tau(t) + G(t) - M\dot{\alpha} + \frac{z_2}{\|z_2\|^2} \Phi(t)) \end{aligned} \quad (19)$$

By virtue of Young's inequality, it follows that

$$z_2^T \Delta f(t-d) \leq \frac{z_2^T z_2}{2} + \frac{1}{2} \Delta f^T(t-d) \Delta f(t-d) \quad (20)$$

And the $\Phi(t)$ can be designed as

$$\Phi(t) = \frac{1}{2} \Delta f^T(t) \Delta f(t) \quad (21)$$

According to the **Assumption 3**, a time delay compensated term τ_{LK} is introduced to compensate the effect caused by time delay.

$$\tau_{LK} = -\frac{\varpi z_2}{\|z_2\|^2} \int_{t-d}^t \frac{\|\bar{f}(s)\|^2}{2} ds \quad (22)$$

Where the ϖ is a designed parameter and the derivation of τ_{LK} will be expressed in the **Stability Analysis** Section.

Remark 2. It should be noted that for τ_{LK} , when $z_2 = 0$ there will be a controller singularity problem. However, as is known to all, the resolution of sensor makes completely equality difficult to achieve. In additional, as is shown in [24], a piecewise approach is provided to avoid the singularity problem while the system reaches origin when $z_2 = 0$. Then the singularity can be solved.

Step 3. Due to the uncertainties of $M, C(v), D(v)$ and $\Phi(t)$ in \dot{z}_2 , RBFNN is introduced to estimate the unknown function:

$$- (C(v) + D(v)) v - M\dot{\alpha} + \frac{z_2}{\|z_2\|^2} \Phi(t) = \Theta^* S(Z) + \varepsilon(Z) \quad (23)$$

Where $Z = (\eta^T, v^T)^T \in \mathbb{R}^6$ is the input vector of NN. $\Theta^* = \begin{pmatrix} \theta_1^{*T} & 0_{1 \times l} & 0_{1 \times l} \\ 0_{1 \times l} & \theta_2^{*T} & 0_{1 \times l} \\ 0_{1 \times l} & 0_{1 \times l} & \theta_3^{*T} \end{pmatrix}^T \in \mathbb{R}^{3l \times 3}$ with $\theta_i^* = (\theta_{i,1}^*, \theta_{i,2}^*, \dots, \theta_{i,l}^*)^T, i = 1, 2, 3$ is

the ideal weight matrix while l is the node number. $S(Z) = (S_1^T(Z), S_2^T(Z), S_3^T(Z))^T \in \mathbb{R}^{3l}$ is the basis functions vector where the $S_i(Z) = (S_{i,1}^T(Z), S_{i,2}^T(Z), \dots, S_{i,l}^T(Z))^T, i = 1, 2, 3$. The basis function vector can be chosen as:

$$S_{ij}(Z) = \exp \left[-\frac{\|Z - c_{ij}\|^2}{b_j^2} \right], i = 1, 2, 3, j = 1, 2, \dots, l \quad (24)$$

where $c_{ij} \in \mathbb{R}^6$ and b_j are the centres and widths of basis functions, respectively. $\varepsilon(Z) = (\varepsilon_1(Z), \varepsilon_2(Z), \varepsilon_3(Z))^T$ is the approximation error vector which satisfies with $\|\varepsilon(Z)\| \leq \bar{\varepsilon}$ and $\bar{\varepsilon}$ is a unknown constant.

Remark 3. Based on Universal Approximation [28], RBFNN can approximate continuous bounded functions with arbitrary precision with the increasing of node number. Theoretically, when the node number l is large enough, the neural network can approach the continuous function with ideal precision on a compact set.

Remark 4. The differentiation of designed virtual control law α can be rewritten as $\dot{\alpha} = \dot{J}^T(\psi)K_1z_1 + J^T(\psi)K_1v(t)$ which can be described by η and v . So the RBFNN with input vector $Z = (\eta^T, v^T)^T$ can approximate $\dot{\alpha}$ and the explosion of complexity can be avoided without constructing first-order filter or command filter.

Remark 5:RBF. neural network is one kind partial approaches network where there is only one hidden layer. The output function of the hidden layer is used to form a set of basis functions to approximate unknown function. Comparing with deep neural network, it has a faster convergence speed since this simple construction.

Step 4. With the increasing of node number of NN, the approximation error is decreasing which is known as Universal Approximation. But it's counterpart, the computational burden is increasing known as "curse of dimensionality". To reduce the computational burden with enough estimated accuracy, the MLP technology is introduced. Considering the following inequality:

$$z_2^T \Theta^{*T} S(\hat{Z}) \leq \frac{\pi \|z_2\|^2 \|S(Z)\|^2}{2} + \frac{1}{2} \quad (25)$$

Where $\pi = \|\Theta^*\|^2$. Designing the adaptive law as:

$$\dot{\hat{\pi}} = \delta_1 \left(\frac{\|z_2\|^2 \|S(Z)\|^2}{2} - \delta_2 (\hat{\pi} - \pi(0)) \right) \quad (26)$$

Where the $\hat{\pi}$ is the estimated value of π and $\pi(0)$ is the initial value of π . δ_1, δ_2 are design parameters.

Step 5. Due to the boundedness of the lumped disturbance $G(t)$ and approximation error $\varepsilon(Z)$, defining $\sigma = \bar{G} + \bar{\varepsilon}$ and a robust adaptive compensated term is designed as:

$$\tau_{RC} = -\frac{z_2}{\|z_2\|} \hat{\sigma} \quad (27)$$

$$\dot{\hat{\sigma}} = \gamma_1 \left(-\gamma_2 \hat{\sigma} + \|\hat{z}_2\| \right) \quad (28)$$

Where the $\hat{\sigma}$ is the estimated value of σ and the initial value $\hat{\sigma}(0) > 0$. γ_1, γ_2 are design positive parameter. τ_{RC} is a robust adaptive term to compensate the unknown time varying disturbance and the unknown saturation.

Step 6. So, the MLP-based robust adaptive controller is constructed as followings

$$\tau(t) = -J^T(\psi)z_1 - K_2z_2 - \frac{\hat{\pi}z_2\|S(Z)\|^2}{2} + \tau_{LK} + \tau_{RC} \quad (29)$$

$$\tau_{RC} = -\frac{z_2}{\|z_2\|} \hat{\sigma} \quad (30)$$

$$\tau_{LK} = -\frac{\varpi z_2}{\|z_2\|^2} \int_{t-d}^t \frac{\|\tilde{f}(s)\|^2}{2} ds \quad (31)$$

$$\hat{\pi} = \delta_1 \left(\frac{\|z_2\|^2 \|S(Z)\|^2}{2} - \delta_2 (\hat{\pi} - \pi(0)) \right) \quad (32)$$

$$\dot{\hat{\sigma}} = \gamma_1 \left(-\gamma_2 \hat{\sigma} + \|\hat{z}_2\| \right) \quad (33)$$

Where the $K_2 \in \mathbb{R}^{3 \times 3}$ is design matrix.

Remark 6. Comparing with the robust adaptive neural networks control in [13], only one parameter needs to be updated online for RBFNN of controller we designed while the computational burden is reduced significantly. Comparing with the conventional MLP controller in [23], a robust adaptive compensator is introduced compensate the error caused by the MLP so that the performance of results are improved.

3.2. Stability analysis

At this point, combining the results in all the six steps previously mentioned, we arrive at the following theorem based on the closed-loop system

Theorem 1:Considering. the dynamic positioning systems (6)~(8), satisfying Assumptions 1~3, the proposed control law (29), and adaptive laws (32) and (33) can guarantees that the closed-loop system uniform ultimately boundedness by choosing appropriate matrix K_1, K_2 and appropriate parameters $\varpi, \delta_1, \delta_2, \gamma_1$ and γ_2 .

Proof. : To prove the ability of closed-loop system, the Lyapunov function candidate can be constructed.

$$V_3 = \frac{1}{2} z_1^T z_1 + \frac{1}{2} z_2^T M z_2 + \frac{1}{2} \tilde{\pi} \delta_1^{-1} \tilde{\pi} + \frac{1}{2\gamma_1} \tilde{\sigma}^2 + \int_{t-d}^t \Phi(s) ds \quad (34)$$

Where $\tilde{\pi} = \hat{\pi} - \pi$ denotes the approximation error of $\|\Theta^*\|^2$ and $\tilde{\sigma} = \hat{\sigma} - \sigma$ denotes the approximation error of adaptive law. Taking the time derivative for V_3

$$\dot{V}_3 = \dot{V}_1 + z_2^T M \dot{z}_2 + \tilde{\pi} \delta_1^{-1} \dot{\hat{\pi}} + \frac{1}{\gamma_1} \tilde{\sigma} \dot{\hat{\sigma}} + \Phi(t) - \Phi(t-d) \quad (35)$$

Substituting (16) and (17) into (35):

$$\begin{aligned} \dot{V}_3 &= -z_1^T K_1 z_1 + z_1^T J(\psi) z_2 + \tilde{\pi} \delta_1^{-1} \dot{\hat{\pi}} + \frac{1}{\gamma_1} \tilde{\sigma} \dot{\hat{\sigma}} + z_2^T (-C(v) + D(v)) \\ &+ \tau(t) + G(t) + \Delta f(t-d) - M\dot{\alpha} + \Phi(t) - \Phi(t-d) \\ &\leq -z_1^T K_1 z_1 + z_1^T J(\psi) z_2 + \tilde{\pi} \delta_1^{-1} \dot{\hat{\pi}} + \frac{1}{\gamma_1} \tilde{\sigma} \dot{\hat{\sigma}} + z_2^T (-C(v) + D(v)) + \tau(t) \\ &+ G(t) + \frac{z_2}{\|z_2\|} \Phi(t) - M\dot{\alpha} + \frac{z_2^T z_2}{2} + \frac{1}{2} f^T(t-d) f(t-d) - \Phi(t-d) \\ &\leq -z_1^T K_1 z_1 + z_1^T J(\psi) z_2 + \tilde{\pi} \delta_1^{-1} \dot{\hat{\pi}} + \frac{1}{\gamma_1} \tilde{\sigma} \dot{\hat{\sigma}} - z_2^T J^T(\psi) z_1 - z_2^T K_2 z_2 + \frac{z_2^T z_2}{2} \\ &- \varpi \int_{t-d}^t \frac{\|\tilde{f}(s)\|^2}{2} ds + z_2^T \left(\Theta^{*T} S(Z) + G(t) + \varepsilon(Z) - \frac{\hat{\pi} z_2 \|S(Z)\|^2}{2} \right. \\ &\left. + \tau_{RC} \right) \end{aligned} \quad (36)$$

Based on the **Assumption 3**, the inequality can be achieved where the τ_{LK} can be designed as Eq. (22) to compensate it:

$$-\varpi \int_{t-d}^t \frac{\|\tilde{f}(s)\|^2}{2} ds \leq -\varpi \int_{t-d}^t \Phi(s) ds \quad (37)$$

Then, based on the inequality (25) and we have:

Table 1
The Main Parameters of The Cybership II.

X_u	-0.7225	Y_v	-10.0
Y_v	-0.8612	N_r	-1.0
Y_r	0.1079	I_z	1.7600
N_r	-0.5	$X_{\dot{u}}$	-2.0
N_v	0.1052	$Y_{\dot{r}}$	0
m	23.8000	X_g	0.0460
$Y_{ v v}$	-36.2823	$N_{\dot{v}}$	0
$X_{ u u}$	-1.3274	$N_{ v v}$	5.0437
X_{uuu}	-5.8664		

$$z_2^T \Theta^{*T} S(Z) \leq \frac{\pi \|z_2\|^2 \|S(Z)\|^2}{2} + \frac{1}{2} \quad (38)$$

So, inequality lie in the (36):

$$\Theta^{*T} S(Z) - \frac{\hat{\pi} z_2 \|S(Z)\|^2}{2} \leq -\frac{\tilde{\pi} z_2 \|S(Z)\|^2}{2} + \frac{1}{2} \quad (39)$$

Substituting adaptive law (32) into (39):

$$\tilde{\pi} \delta_1^{-1} \dot{\hat{\pi}} = \tilde{\pi} \left(\frac{\|z_2\|^2 \|S(Z)\|^2}{2} - \delta_2 (\hat{\pi} - \pi(0)) \right) \quad (40)$$

Considering the right part of (40):

$$\begin{aligned} & -\delta_2 \tilde{\pi} (\hat{\pi} - \pi(0)) \\ &= -\delta_2 \tilde{\pi}^2 - \delta_2 \tilde{\pi} (\pi - \pi(0)) \\ &\leq -\delta_2 \tilde{\pi}^2 + \frac{1}{2} \delta_2 \tilde{\pi}^2 + \frac{1}{2} \delta_2 (\pi - \pi(0))^2 \\ &\leq -\frac{\delta_2}{2\lambda_{\max}(\delta_1^{-1})} \tilde{\pi} \delta_1^{-1} \tilde{\pi} + \frac{1}{2} \delta_2 (\pi - \pi(0))^2 \end{aligned} \quad (41)$$

Considering the inequalities (39) and (41), we have:

$$\Theta^{*T} S(Z) - \frac{\hat{\pi} z_2 \|S(Z)\|^2}{2} + \tilde{\pi} \delta_1^{-1} \dot{\hat{\pi}} \leq -\frac{\delta_2}{2\lambda_{\max}(\delta_1^{-1})} \tilde{\pi} \delta_1^{-1} \tilde{\pi} + \frac{1}{2} + \frac{1}{2} \delta_2 (\pi - \pi(0))^2 \quad (42)$$

Next, considering the robust adaptive compensated terms:

$$z_2^T (G(t) + \varepsilon(Z) + \tau_{RC}) \leq \|z_2\| (\sigma - \hat{\sigma}) \quad (43)$$

Based on the adaptive law:

$$\frac{1}{\gamma_1} \dot{\hat{\sigma}} = -\gamma_2 \tilde{\sigma} \hat{\sigma} + \tilde{\sigma} \|z_2\| \quad (44)$$

Combining the (43) and (44), we have:

$$\begin{aligned} & z_2^T (G(t) + \varepsilon(Z) + \tau_{RC}) + \frac{1}{\gamma_1} \dot{\hat{\sigma}} \\ &\leq -\|z_2\| \tilde{\sigma} - \gamma_2 \tilde{\sigma} \hat{\sigma} + \tilde{\sigma} \|z_2\| \\ &= -\gamma_2 \tilde{\sigma} \hat{\sigma} \end{aligned} \quad (45)$$

In the light of following inequalities:

$$2\tilde{\sigma} \hat{\sigma} = \tilde{\sigma}^2 + \hat{\sigma}^2 - \sigma^2 \geq \tilde{\sigma}^2 - \sigma^2 \quad (46)$$

The (45) can be written as:

$$-\gamma_2 \tilde{\sigma} \hat{\sigma} \leq -\frac{\gamma_2 \tilde{\sigma}^2}{2} + \frac{\gamma_2 \sigma^2}{2} \quad (47)$$

Substituting (47) into (45), it follows:

$$z_2^T (G(t) + \varepsilon(Z) + \tau_{RC}) + \frac{1}{\gamma_1} \dot{\hat{\sigma}} \leq -\frac{\gamma_2 \tilde{\sigma}^2}{2} + \frac{\gamma_2 \sigma^2}{2} \quad (48)$$

So, substituting (37), (42) and (48) into (36), the differential of V_3 can be rewritten as:

$$\begin{aligned} \dot{V}_3 &\leq -z_1^T K_1 z_1 - z_2^T \left(K_2 - \frac{1}{2} I_{3 \times 3} \right) z_2 - \varpi \int_{t-d}^t \Phi(s) ds \\ &\quad - \frac{\delta_2}{2\lambda_{\max}(\delta_1^{-1})} \tilde{\pi} \delta_1^{-1} \tilde{\pi} + \frac{1}{2} + \frac{1}{2} \delta_2 (\pi - \pi(0))^2 - \frac{\gamma_2 \tilde{\sigma}^2}{2} + \frac{\gamma_2 \sigma^2}{2} \\ &\leq -\mu V_3 + \rho \end{aligned} \quad (49)$$

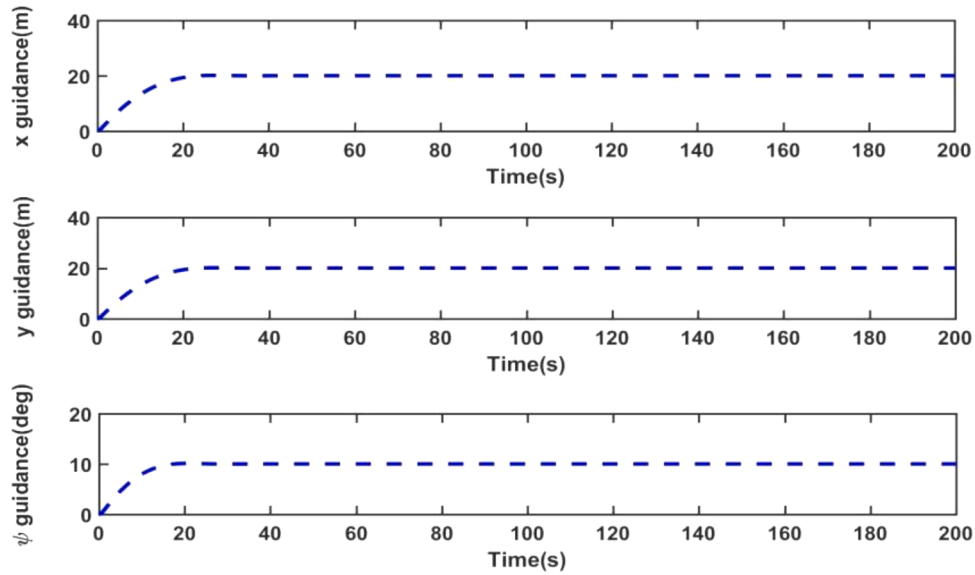


Fig. 1. The desired positions and heading in surge, sway and yaw generated by guidance law. (For interpretation of the references to colour in this figure legend, the reader is referred to the web version of this article.)

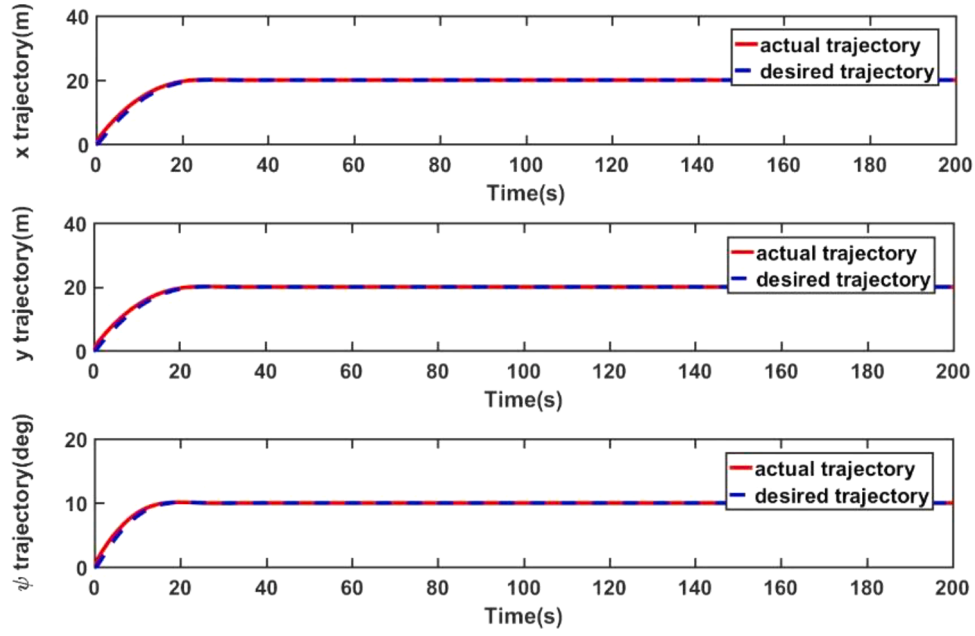


Fig. 2. The curve of DP in surge, sway and yaw.

Where $\mu = \min \left\{ 2\lambda_{\min}(K_1), 2\lambda_{\min} \left[\left(K_2 - \frac{1}{2}I_{3 \times 3} \right) M^{-1} \right], \frac{\delta}{\lambda_{\max}(\delta_1^{-1})}, \frac{\gamma_1 \gamma_2}{2}, \varpi \right\}, \rho$
 $= \frac{1}{2} + \frac{\gamma_2}{2}\sigma^2 + \frac{1}{2}\delta_2(\pi - \pi(0))^2$. Integrating (49), we have:

$$0 \leq V_3(t) \leq \frac{\rho}{2\mu} + \left[V_3(0) - \frac{\rho}{2\mu} \right] e^{-2\mu t} \quad (50)$$

Therefore, $V_3(t)$ is globally uniformly ultimately bounded. Then, according to (34) and (50), we can obtain:

$$\|z_1\| \leq \sqrt{\frac{\rho}{\mu} + 2 \left[V_3(0) - \frac{\rho}{2\mu} \right] e^{-2\mu t}} \quad (51)$$

Obviously, the error of position z_1 is globally uniformly ultimately bounded. For any positive constant $\varsigma > \sqrt{\rho/\mu}$, there exists a time constant $T > 0$ such that $\|z_1\| \leq \varsigma$ for all $t > T$. Thus, z_1 settles within $\Omega_{z_1} = \{z_1 \in \mathbb{R}^3 \mid \|z_1\| \leq \varsigma\}$ which can be made arbitrarily small by appropriately selecting $K_1, K_2, \varpi, \Gamma, \delta, \gamma_1$ and γ_2 . Hence, the ship can be maintained at

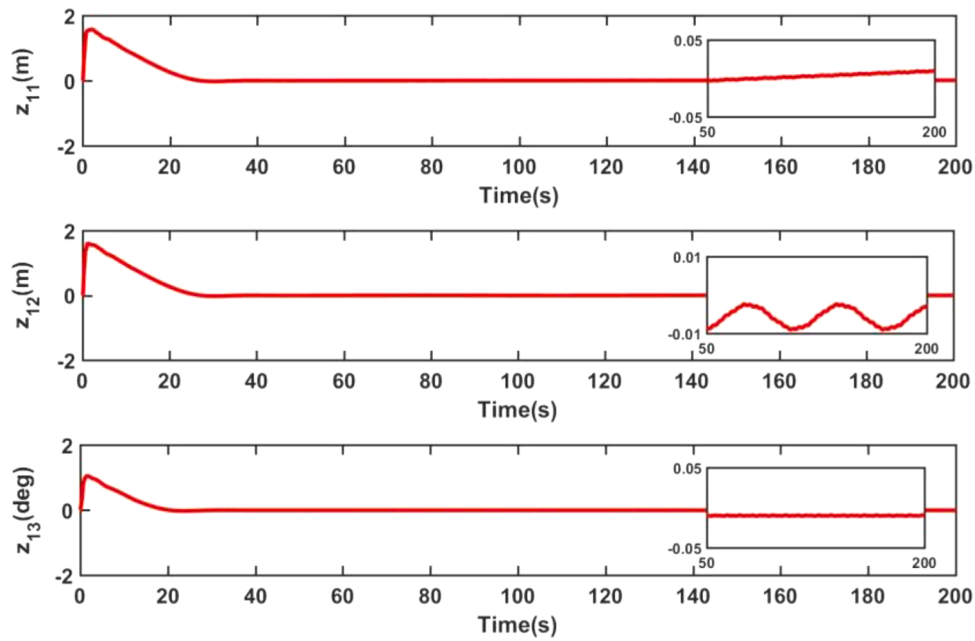


Fig. 3. The errors between guidance law and actual trajectory.

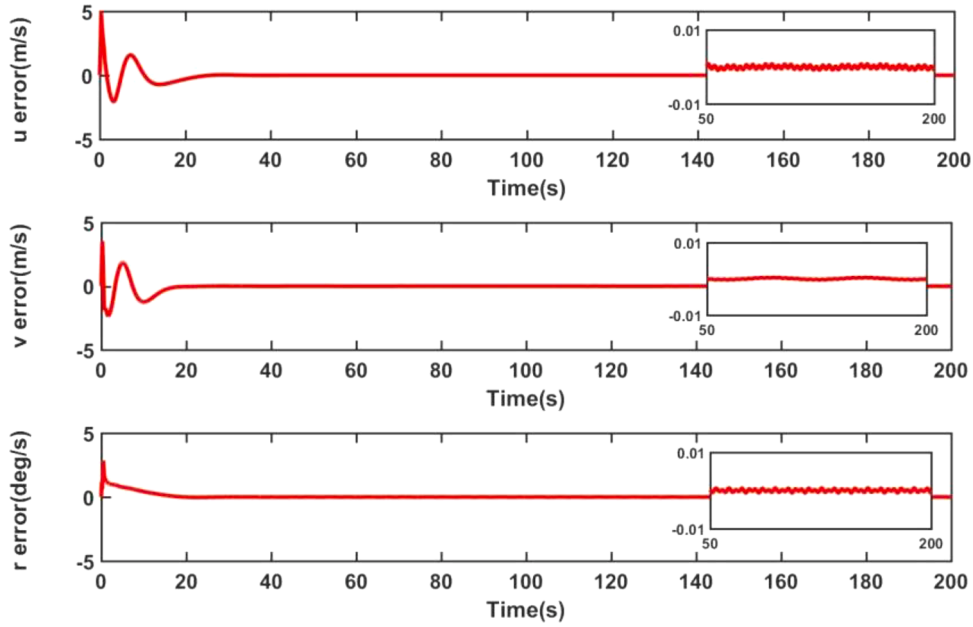
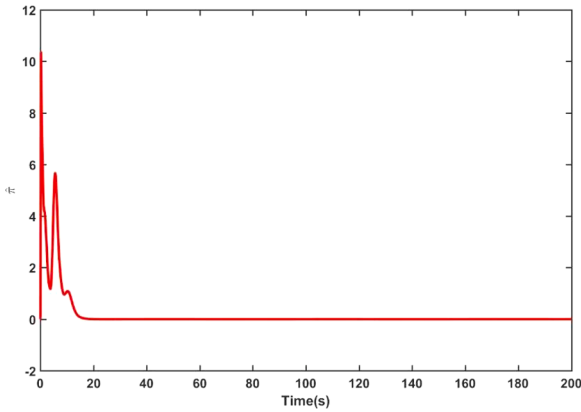


Fig. 4. The curve of velocities.

Fig. 5. The norm of $\hat{\pi}$.

the desired position and heading with arbitrarily small errors. **Theorem1** is thus proved.

4. Simulations

4.1. Simulation setting

In order to present that the proposed control strategy in the previous section work effectively, numerical simulations tested on a supply vessel called CyberShip II [29], which is a 1:70 scale-replica of a supply ship whose main parameters is shown in Table 1, are performed and the results are shown in this section. The actuator input limitation [30] is set as $|\tau_{imax}| = 50$. The unknown external disturbances [31] τ_d with significantly large magnitude and high frequency, which can be roughly considered as complex environment including ocean winds, waves, and currents, are governed by

$$\tau_d = \begin{pmatrix} -2\cos(0.5t)\cos(t) + 0.3\cos(0.5t)\sin(0.5t) - 3 \\ 0.01\sin(0.1t) \\ 0.6\sin(1.1t)\cos(0.3t) \end{pmatrix}$$

Assuming the uncertainties containing delay states [26]:

$$f(t) = \begin{pmatrix} 0.5(\sin(x) + \cos(\mu)) \\ 0.4(\sin(y) - \cos(v)) \\ 0.2(\sin(\psi) - \cos(r)) \end{pmatrix}$$

With initial conditions $\eta_d = [0m, 0m, 0^\circ]^T$ and desired position is $[20m, 20m, 10^\circ]^T$. In order to generate smoothly desired path, the 2-order filter [22] is applied as

$$\begin{cases} \dot{\eta}_d = v_d \\ \ddot{\eta}_d = -\omega_n^2 \eta_d - \chi |\eta_d| \eta_d - 2\zeta \omega_n \dot{\eta}_d + \omega_n^2 \eta_p \end{cases}$$

Where $\dot{\eta}_d, \ddot{\eta}_d \in \mathbb{R}^3$ is the first derivative and second derivative of desired position, respectively, ω_n is the natural frequency, ζ is the relative damping ratio, δ is the designed parameter, η_p is input signal. Selecting $\omega_n = 0.4, \zeta = 0.5, \chi = 0.8, \eta_p = [20, 20, 10]^T$, and the trajectory generated by guidance law is showed in Fig. 1.

Choosing the node number $l = 500$, width $b_j = 2, j = 1, 2, \dots, l$ and centers c_{ij} ($i = 1, 2, \dots, 6, j = 1, 2, \dots, l$) evenly spaced in:

$$[-2 \ 20] \times [-2 \ 20] \times [-0.1 \ 0.2] \times [-2 \ 1] \times [-0.02 \ 0.01], \delta_1 = 1, \delta_2 = 1, \pi(0) = 0, \gamma_1 = 15, \gamma_2 = 30, K_1 = \text{diag}\{40, 50, 20\}, K_2 = \text{diag}\{50, 50, 50\}.$$

To demonstrate the superiority and validity, a scenario as comparative case is provided here.

Scenario1: Conventional Controller in [22]

In [22], a fuzzy controller is proposed to handle with the uncertainties and time delay in which two drawbacks lies. Here, based on the approach in [22], a MLP-based RBFNN controller is provided as comparative case to demonstrate the superiority of our controller. The

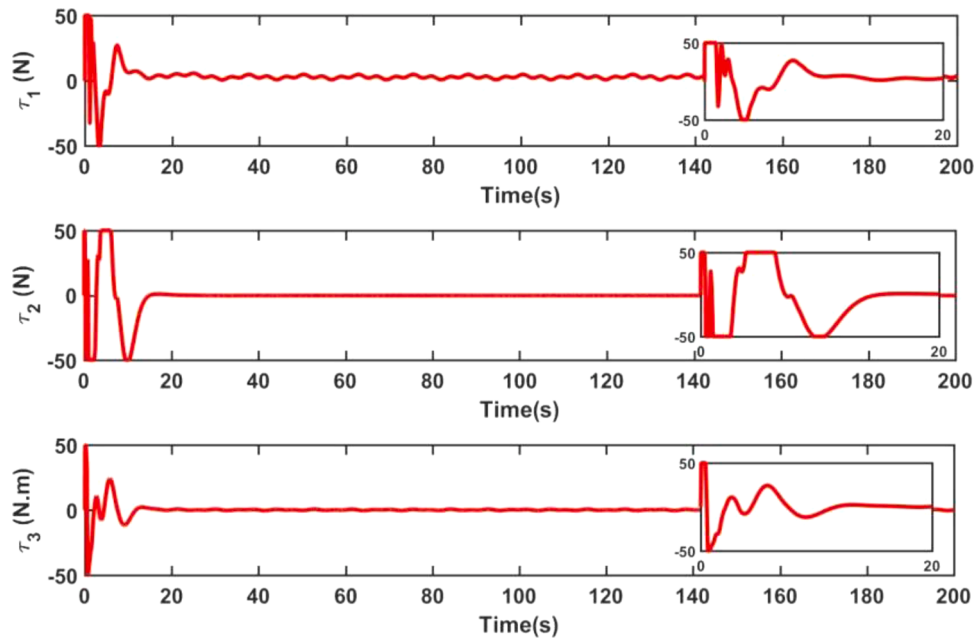


Fig. 6. The control input signal.

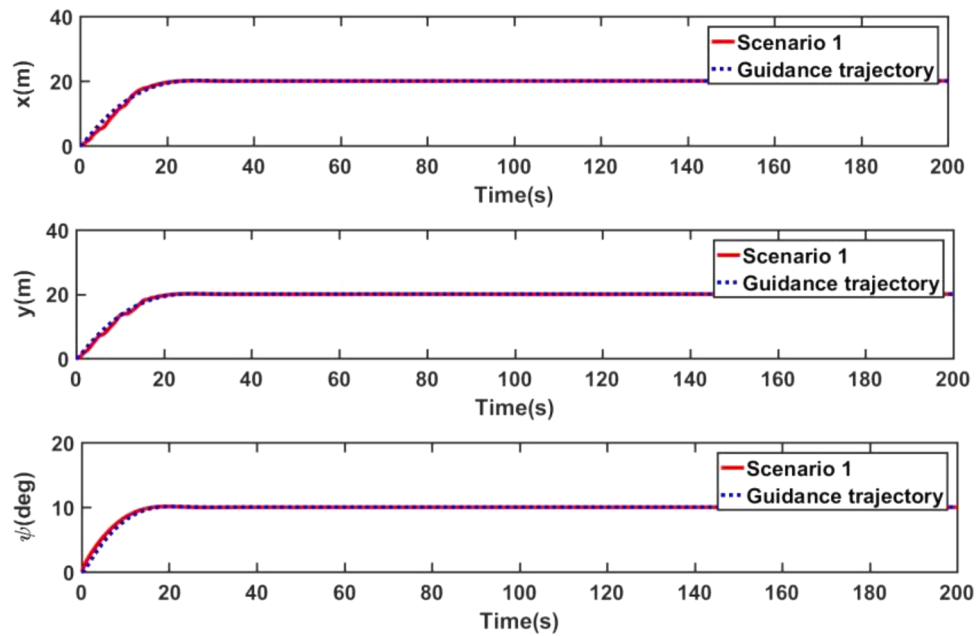


Fig. 7. The desired trajectory and actual trajectory in **Scenario 1**. (For interpretation of the references to colour in this figure legend, the reader is referred to the web version of this article.)

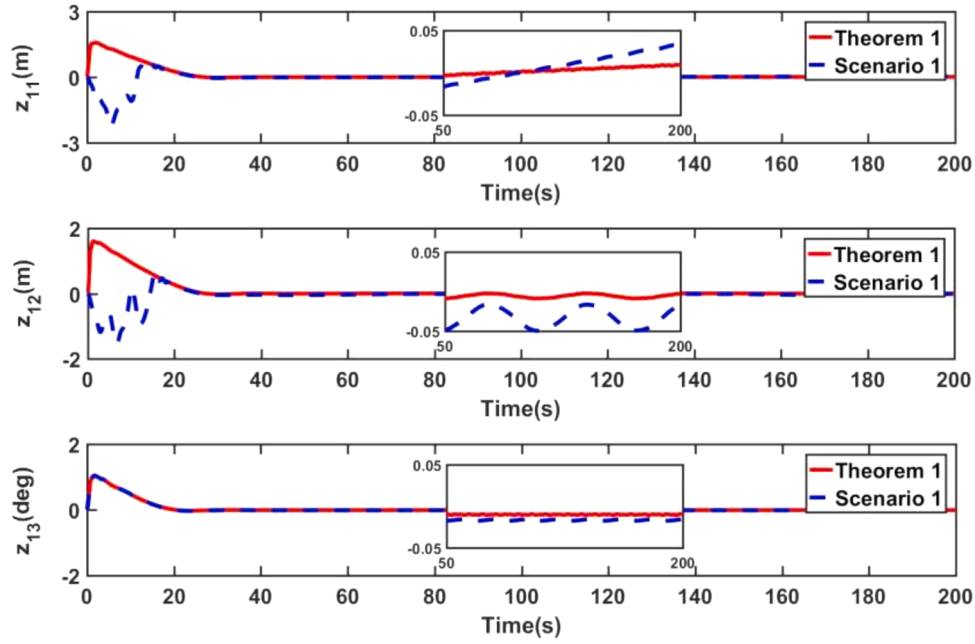


Fig. 8. The comparison of trajectory errors in position and yaw.

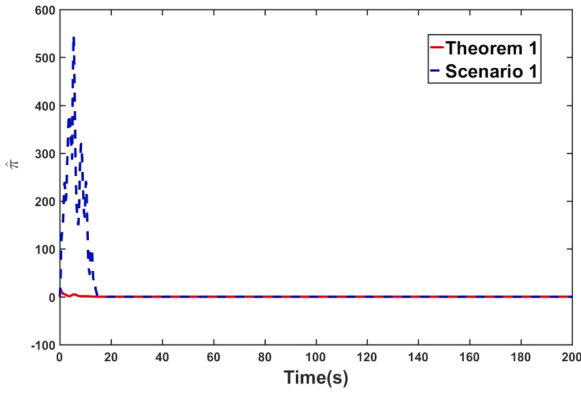


Fig. 9. The norm of $\hat{\pi}$ between the **Scenario 1** and **Theorem 1**.

MLP-based RBFNN is designed as following.

$$\tau_{C1} = -J^T(\psi)z_1 - K_2z_2 - \frac{\hat{\pi}z_2\|S(Z)\|^2}{2} + \tau_{LK} \quad (52)$$

$$\tau_{LK} = -\frac{\omega z_2}{\|z_2\|^2} \int_{t-d}^t \frac{\|\bar{f}(s)\|^2}{2} ds \quad (53)$$

$$\dot{\hat{\pi}} = \delta_1 \left(\frac{\|z_2\|^2\|S(Z)\|^2}{2} - \delta_2(\hat{\pi} - \pi(0)) \right) \quad (54)$$

Scenario2: An adaptive MLP-based RBFNN Controller without input constraint

To show the improvement comparing with the MLP-based without input constraint, a MLP-based controller without input constraint simulation is provided. In this case, the controller is designed as (52)~(54) while the input signal can be provided without constraint.

4.2. Numerical simulations

At first, the effectiveness of control law we design is confirmed from Fig. 2~ Fig. 6 and it shows that the controller we designed can guarantee the dynamic positioning of ship maintain at the desired position smoothly with arbitrarily small errors. As it's showed in Fig. 2, which provides the actual trajectory of ship and the desired trajectory in surge, sway and yaw respectively, the ship reaches the desired point and attitude smoothly, while the steady error can be maintained within $0.05m$, $0.01m$ and $0.05deg$, respectively, which shows in Fig. 3. It can be concluded that the controller we designed can achieve the object proposed in Section 2 considering time delay, unknown input saturation, unknown time-varying disturbances and dynamic uncertainties, simultaneously. In Fig. 4, the curves of velocities in surge, sway and yaw are given where we can find that the velocities change smoothly and are steady since ship reach the desired point. To be more specific, the velocities of ship are maintained within $0.01m/s$, $0.01m/s$ and $0.01deg/s$, respectively, which means that the dynamic positioning of ship will locate at the desired point steadily. The updated progress of $\hat{\pi}$ is showed in Fig. 5 and the Fig. 6 shows the input signal with constraint. In particular, only one parameter needs to be updated online for RBFNN of controller we designed while 1500 parameters needs to be updated in conventional approach [11]. Hence, the computational burden is reduced significantly with high precision. In the designing of controller, the problem of “explosion of complexity” in the conventional backstepping method and “curse of dimensionality” in the traditional neural networks control are avoided without additional equipment which makes it easy to be implemented in practical engineering.

Figs. 7~10 gives the comparison between controller we designed in Theorem 1 and existing controller given by Scenario 1. As showed in Fig. 7, the controller of Scenario 1 can guarantee the ship locate at the desired point while there are shocks in the progress of positioning which caused by the control constraint as showed in Fig. 10. It can be find in

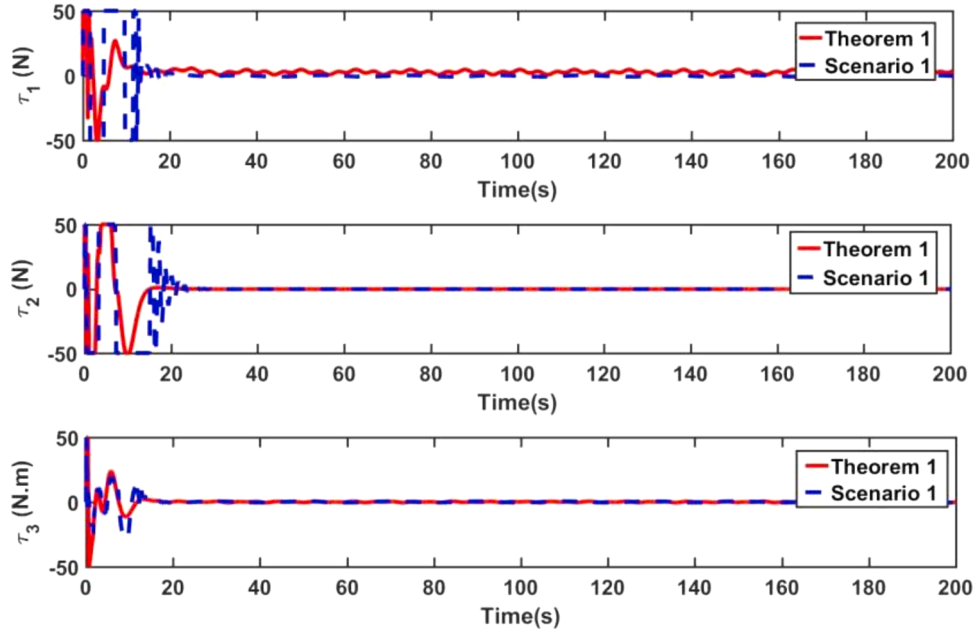


Fig. 10. The comparison of input signal.

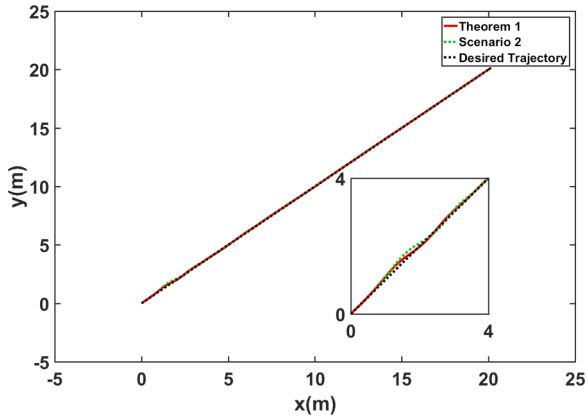


Fig. 11. The comparison of trajectory between Theorem 1 and Scenario 2.

Figs. 9–10 that the input saturation can't be compensated during the initial stage which makes the transient performance worse and the shocks during the convergence of $\hat{\pi}$. In addition, it can be find in Fig. 8 that the positioning error after ship reach the desired point is bigger than the controller we design which means **Theorem 1** achieve better steady performance. Comparing with the **Scenario 1**, the controller designed in **Theorem 1** deal with the input saturation and the approximation error caused by MLP-based RBFNN where a robust adaptive compensated term is introduced to handle with them. So the robustness is improved comparing with the traditional MLP-based controller at low cost of computational burden. On one hand, the problem of transient performance degradation caused by input saturation is improved; on the other hand, the problem of steady error caused by approximation error of neural network is solved. In conclusion, compared with the existing control algorithms, the controller we proposed has better transient performance and steady-state performance.

Figs. 11–12 show the comparison between controller we designed in **Theorem 1** and comparing case set in **Scenario 2**. As showed in Fig. 11, the controller of Scenario 2 can guarantee the ship locate at the desired point while there are shocks in the initial stage where it's worse than the results provided by **Theorem 1** although there are no constraints for input magnitude in **Scenario 2** while there are constraints in **Theorem 1**. Comparing with the results of **Theorem 1**, the robust adaptive compensated term is introduced to deal with approximation error caused by MLP-based RBFNN while the robustness of MLP-based method is improved. As is shown in Fig. 13, the input dynamic positioning ship needed in **Scenario 2** is larger than the input energy needed by controller in **Theorem 1** dramatically which means a better performance can be achieved by the controller we designed in this paper while the input energy can be reduced significantly.

5. Conclusion

In this paper, a MLP-based robust adaptive RBFNN controller, through incorporating robust adaptive compensated technology, MLP technology, Lyapunov – Krasovskii theory and RBFNN into backstepping control, is proposed for dynamic positioning of ship in present of the unknown input saturation, time delay, unknown time-varying disturbances and dynamic uncertainties. An appropriate Lyapunov-Krasovskii Function (LKF) is constructed to overcome the effect caused by time-delay and the MLP technology is applied to reduce the computational burden while the problems of “explosion of complexity” and “curse of dimensionality” are avoided which will make it easy to apply the controller in practical engineering. In particular, a robust adaptive compensate term is introduced to estimate the bound of the lumped disturbance including the unknown saturation, unknown external disturbance and the approximate error of neural networks control while the robustness of RBFNN with MLP is improved while the prior knowledge of input saturation is not required. The simulations demonstrate that, compared with the existing control algorithms, the controller we proposed has better transient performance and steady-state

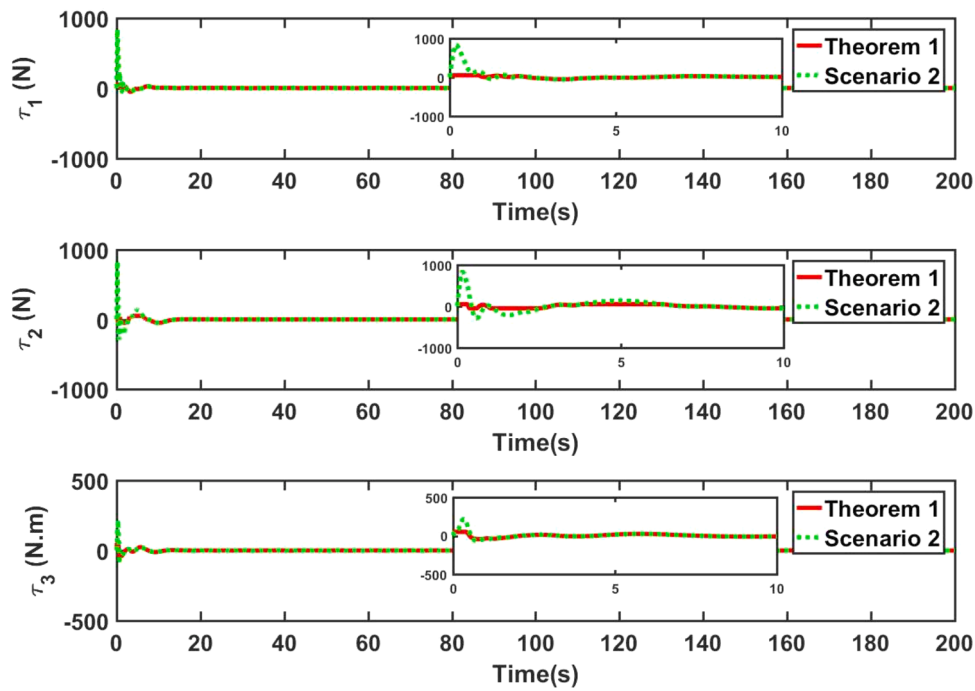


Fig. 12. The comparison of input between **Theorem 1** and **Scenario 2**.

performance. In further study, the approaches to estimate the delay time should be addressed [32] and new intelligent control should be introduced [33]. In additional, it will be interesting to consider control to improve the transient performance and the ability against disturbance [34–40].

Supplementary materials

All the data supporting the conclusions of the study have been provided in the Simulations section and readers can access these data in [29–31].

CRediT authorship contribution statement

Kun Liang: Conceptualization, Methodology, Funding acquisition, Formal analysis, Writing - original draft. **Xiaogong Lin:** Resources, Supervision, Project administration. **Yu Chen:** Visualization, Writing - review & editing. **Yeye Liu:** Investigation, Writing - review & editing. **Zhaoyu Liu:** Data curation, Software. **Zhengxiang Ma:** Funding acquisition. **Wenli Zhang:** Writing - review & editing.

Declaration of Competing Interest

None

Acknowledgements

This research was funded by the Science and Technology Project of Henan Province (Project nos. 202102210137, 202102210315), and the National Science Technology Support Program of China (Project nos. 62073297, 51609046, 51975539).

References

- Shi, Y., Shen, C., Fang, H.Z., Li, H.P., 2017. Advanced control in marine mechatronic systems: a survey. *IEEE/ASME Trans. Mechatron.* 22 (3), 1121–1131.
- Hu, X., Du, J.L., Sun, Y.Q., 2017. Robust adaptive control for dynamic positioning of ships. *IEEE J. Oceanic Eng.* 42 (4), 1–10.
- Nguyen, T.D., Queka, R.T., 2007. Design of hybrid controller for dynamic positioning from calm to extreme sea conditions. *Automatica* 43 (5), 768–785.

- Du, J.L., Hu, X., Krstić, M., Sun, Y.Q., 2016. Robust dynamic positioning of ships with disturbances under input saturation. *Automatica* 73, 207–214.
- Lin, Y.Y., Du, J.L., Zhu, G.B., Fang, H.Z., 2018. Thruster fault-tolerant control for dynamic positioning of vessels. *Appl. Ocean Res.* 80, 118–124.
- Sørensen, A.J., 2011. A survey of dynamic positioning control systems. *Annu. Rev. Control* 35 (1), 123–136.
- Hussain, M., Rehan, M., Ahmed, S., Abbas, Tanveer, Tufail, M., 2020. A novel approach for static anti-windup compensation of one-sided Lipschitz systems under input saturation. *Appl. Math. Comput.* 380, 125229.
- [8] Rehman, A.U., Rehan, M., Mehar, M.R., Abid, M., Iqbal, N., 2020. Consensus tracking of nonlinear multi-agent systems under input saturation with applications: a sector-based approach. *ISA Trans* 107, 194–205.
- Su, Y.X., Zheng, C.H., Mercorelli, P., 2016. Nonlinear PD fault-tolerant control for dynamic positioning of ships with actuator constraints. *IEEE/ASME Trans. Mechatron.* 22 (3), 1132–1142.
- Hu, X., Du, J.L., 2018. Robust nonlinear control design for dynamic positioning of marine vessels with thruster system dynamics. *Nonlinear Dynam* 94, 365–376.
- Perez, T., Donaire, A., 2009. Constrained control design for dynamic positioning of marine vehicles with control allocation. *Model. Ident. Control* 30 (2), 57–70.
- Do, K.D., 2011. Global robust and adaptive output feedback dynamic positioning of surface ships. *J. Mar. Sci. Appl.* 10, 325–332.
- [13] Du, J.L., Yang, Y., Wang, D.H., Guo, C., 2013. A robust adaptive neural networks controller for maritime dynamic positioning system. *Neurocomputing* 110, 128–136.
- [14] Hu, X., Du, J.L., Zhu, G.B., Sun, Y.Q., 2018. Robust adaptive NN control of dynamically positioned vessels under input constraints. *Neurocomputing* 318, 201–212.
- Liang, K., Lin, X.G., Chen, Y., Li, J., Ding, F.G., 2020. Adaptive sliding mode output feedback control for dynamic positioning ships with input saturation. *Ocean Eng.* 206, 107245.
- Liang, K., Lin, X.G., Chen, Y., Zhang, W.L., Li, J., 2021. Robust adaptive multistage anti-windup dynamic surface control for dynamic positioning ships with mismatched disturbance. *J. Franklin I.* <https://doi.org/10.1016/j.jfranklin.2021.01.003>.
- Vahidi-Moghaddam, A., Rajaei, A., Ayati, M., 2019. Disturbance-observer-based fuzzy terminal sliding mode control for MIMO uncertain nonlinear systems. *Appl. Math. Model.* 70, 109–127.
- Chen, M., Wu, Q.X., Cui, R.X., 2013. Terminal sliding mode tracking control for a class of SISO uncertain nonlinear systems. *ISA Trans* 52 (2), 198–206.
- Hao, L.Y., Zhang, H., Li, H., Li, T.S., 2020. Sliding mode fault-tolerant control for unmanned marine vehicles with signal quantization and time-delay. *Ocean Eng* 215, 107882.
- Lei, Z.L., Guo, C., 2015. Disturbance rejection control solution for ship steering system with uncertain time delay. *Ocean Eng* 95, 78–83.
- Lin, X.G., Liang, K., Li, H., Jiao, Y.Z., Nie, J., 2018. Robust finite-time h-infinity control with transients for dynamic positioning ship subject to input delay. *Math. Probl. Eng.*, 2838749.
- Xia, G.Q., Xue, J.J., Jiao, J.P., 2018. Dynamic positioning control system with input time-delay using fuzzy approximation approach. *Inter. J. Fuzzy Syst.* 20 (2), 630–639.

- 23 Zhang, G.Q., Huang, C.F., Zhang, X.K., Zhang, W.D., 2018. Practical constrained dynamic positioning control for uncertain ship through the minimal learning parameter technique. *IET Control Theory Appl* 12 (18), 2526–2533.
- [24] Chen, Y.H., Yang, X.B., Zheng, X.L., 2018. Adaptive Neural Control of a 3-DOF Helicopter with Unknown time delay. *Neurocomputing* 307 (13), 98–105.
- 25 Sui, S., Chen, C.L.P., Tong, S.C., 2019. Neural Network Filtering Control Design for Nontriangular Structure Switched Nonlinear Systems in Finite Time. *IEEE Trans. Neur. Net. Lear.* 30 (7), 2153–2162.
- 26 Cai, J.P., Wan, J., Que, H.Y., Zhou, Q.P., Shen, L.J., 2018. Adaptive actuator failure compensation control of second-order nonlinear systems with unknown time delay. *IEEE Access* 6 (99), 15170–15177.
- 27 I., T., 2012. *Fossen Handbook of Marine Craft Hydrodynamics and Motion Control*. John Wiley, Norway.
- 28 Park, J., Sandberg, I.W., 1991. Universal approximation using radial-basis-function networks. *Neural Comput.* 3 (2), 246–257.
- 29 Skjetne, R., Fossen, T.I., Kokotović, P.V., 2005. Adaptive maneuvering, with experiments, for a model ship in a marine control laboratory. *Automatica* 41 (2), 289–298.
- 30 Fu, M.Y., Yu, L.L., 2018. Finite-time extended state observer-based distributed formation control for marine surface vehicles with input saturation and disturbances. *Ocean Eng.* 159, 219–227.
- 31 Lu, Y., Zhang, G.Q., Sun, Z.J., Zhang, W.D., 2018. Adaptive cooperative formation control of autonomous surface vessels with uncertain dynamics and external disturbances. *Ocean Eng.* 167, 36–44.
- 32 Haus B, B., Mercorelli, P., 2019. An extended Kalman filter for time delays inspired by a fractional order model. *Lect. Notes Electr. Eng.* 496, 151–163.
- [33] Sui, S., Chen, C.L.P., Tong, S.C., Feng, S., 2020. Finite-time adaptive quantized control of stochastic nonlinear systems with input quantization: a BLS-based identification method. *IEEE Trans. Ind. Electron.* 67 (6), 8555–8565.
- 34 Mironova, A., Mercorelli, P., Zedler, A., 2017. A multi input sliding mode control for peltier cells using a cold-hot sliding surface. *J. Franklin I.* 355 (18), 9351–9373.
- 35 Hu, X., Du, J.L., Shi, J.W., 2015. Adaptive fuzzy controller design for dynamic positioning system of vessels. *Appl. Ocean Res.* 53, 46–53.
- 36 Yin, S., Xiao, B., 2017. Tracking control of surface ships with disturbance and uncertainties rejection capability. *IEEE/ASME Trans. Mechatron.* 22 (3), 1154–1162.
- 37 Wang, N., Qian, C., Sun, J.C., Liu, Y.C., 2016. Adaptive robust finite-time trajectory tracking control of fully actuated marine surface vehicles. *IEEE Trans. Contr. Syst. Tech.* 24 (4), 1454–1462.
- 38 Hu, X., Wei, X.J., Han, J., Zhang, Q., 2020. Adaptive disturbance rejection for course tracking of marine vessels under actuator constraint. *ISA Trans* 100, 82–91.
- 39 Su, Y.X., Zheng, C.H., Mercorelli, P., 2017. Global Finite-Time Stabilization of Planar Linear Systems With Actuator Saturation. *IEEE Trans. Circuits II* 64 (8), 947–951.
- 40 Sui, S., Tong, S.C., Chen, C.L.P., 2018. Finite-time filter decentralized control for nonstrict-feedback nonlinear large-scale systems. *IEEE Trans. Fuzzy Syst.* 26 (6), 3289–3300.